

Kinetics of oxalic acid leaching of tincal

Y. Abali^a, S.U. Bayca^{b,*}, E. Mistincik^a

^a Department of Chemistry, Faculty of Science and Art, Celal Bayar University, Manisa, Turkey

^b Soma Technical and Vocational School, Celal Bayar University, Soma, Manisa, Turkey

Received 8 April 2006; received in revised form 10 July 2006; accepted 12 July 2006

Abstract

The leaching kinetics of tincal in oxalic acid solutions was investigated in this study. The effects of parameters reaction temperature, acid concentration, solid to liquid ratio, particle size and stirring speed on tincal leaching were determined in the experiments. It is observed that the leaching rate increases with increasing reaction temperature, stirring speed and decreasing solid to liquid ratio and particle size. The experimental data tested the reaction control models and the best model for the leaching rates of tincal was the product layer model. The activation energy of the process was calculated as 35.14 kJ mol⁻¹.

© 2006 Elsevier B.V. All rights reserved.

Keywords: Tincal; Leaching; Kinetic model; Oxalic acid; Reaction control process; Borax

1. Introduction

Boron compounds are used in the manufacturing of a variety of industrial products including advanced minerals. Although boron is widely used in industry, it is not widely distributed around the world. Turkey has 63% of the world's total boron reserves. Tincal (borax) is a sodium borate mineral. The world's largest deposits are located in Eskişehir's Kırka district [1]. Sodium tetraborate decahydrate, borate, tincal, Na₂B₄O₇·10H₂O, crystals are odorless, white, monoclinic prisms with a relative density of 1.715 [2]. Boric acid is produced commercially by reactions of sulphuric acid with sodium borate in the United States, with colemanite in Europe and Turkey [3]. Boric acid has a surprising variety of applications in both industrial and consumer products. It serves as a source of B₂O₃ in many fused products, including textile fiberglass, optical and sealing glasses, heat resistant borosilicate glass, ceramic glazes and porcelain enamels. It also serves as a component of fluxes for welding and brazing [4].

Many studies have been carried out on the dissolution kinetics of colemanite and ulexite to produce boric acid. Kocakerim et al. [5] have studied the dissolution kinetics of colemanite in SO₂ saturated water. The activation energy was calculated as 53.97 kJ mol⁻¹. Alkan et al. [6] have conducted the dissolution

kinetics of inyoite and inderite in CO₂ saturated water. The activation energy was calculated as 58.50 kJ mol⁻¹ for inyoite, and 61.30 kJ mol⁻¹ for inderite. Kum et al. [7] investigated the dissolution kinetics of calcined colemanite in ammonium chloride solution. The activation energy for the dissolution of the calcined colemanite at 400 °C was found to be 89 kJ mol⁻¹. Özmetin et al. [8] have investigated the dissolution kinetic of colemanite in aqueous acetic acid solutions. The activation energy for process was determined 51.49 kJ mol⁻¹. Kunkul et al. [9] have studied the dissolution kinetics of ulexite in ammonia solutions saturated with CO₂. It was found that the dissolution rate of ulexite can be described by a first-order pseudo-homogenous reaction model.

In recent years, the dissolution kinetics of colemanite (2CaO·3B₂O₃·5H₂O) and ulexite (Na₂O·CaO·5B₂O₃·16H₂O) in acid solutions has been investigated. The dissolution kinetics of colemanite in oxalic acid [10], phosphoric acid [11] and acetic acid [12] solutions has been studied. The dissolution kinetics of colemanite has been determined to conform to product layer control model in oxalic acid, chemical reaction control model in phosphoric acid, and first order pseudohomogenous control model in acetic acid. The activation energy of colemanite using these models was estimated to be 39.71 kJ mol⁻¹ in oxalic acid, 53.91 kJ mol⁻¹ in phosphoric acid and 51.49 kJ mol⁻¹ in acetic acid solutions.

The dissolution kinetics of ulexite in oxalic acid [13], in sulphuric acid [14], and in acetic acid [15] solutions has been studied. The dissolution kinetics of ulexite has been determined to

* Corresponding author. Tel.: +90 236 612 0063; fax: +90 236 612 2002.
E-mail address: salih.bayca@bayar.edu.tr (S.U. Bayca).

conform to first order pseudohomogenous control model, product layer control model, and product layer control model, respectively. The activation energy of ulexite using these models was estimated to be $30.69 \text{ kJ mol}^{-1}$ in oxalic acid and $30.10 \text{ kJ mol}^{-1}$ in acetic acid solutions.

Present study investigates the leaching kinetics of tincal in oxalic acid solutions. The effects of reaction temperature, acid concentration, solid to liquid ratio, stirring speed, and particle size on leaching rate of tincal in oxalic acid were determined. Leaching rates were tested using the reaction control models to determine the best model. Activation energy was also calculated by using the best model equations and Arrhenius equation.

2. Experimental procedure

The tincal used in these experiments was obtained from Eti Mine Kirka Boron Works Eskişehir, Turkey. Tincal was crushed by jaw crusher. The sample was sieved by using ASTM Standard sieves to obtain a particle size fraction of 160–900 μm . The chemical and X-ray diffraction analyses of the sample are given in Table 1 and in Fig. 1, respectively. As can be seen in Fig. 1 the sample mainly composed of tincal and dolomite in a lesser proportion. Oxalic acid was obtained from Merck Co.

The leaching experiments were performed in a 250 mL glass reactor at atmospheric pressure. A mechanical stirrer was used and a thermostat was employed to keep the reaction medium at constant temperature. In the leaching process, 100 mL of oxalic acid solution was put into the reactor. After the desired reaction temperature was reached, a specific amount of the sample was added to the solution and the stirring started. After a certain period of time, the solution was filtered without any decrease in temperature. The amount of B_2O_3 in the filtrate was determined

Table 1
Chemical characteristics of used material

Content	Percent
B_2O_3	34.3
Na_2O	16.3
Others	4.8
H_2O	44.5

Table 2
Parameters and their values corresponding to their levels

Parameters	Levels				
	1	2	3	4	5
Reaction temperature ($^{\circ}\text{C}$)	20	30	40	50	–
Acid concentration (% w/v)	1	2	3	5	10
Solid to liquid ratio (% w/v)	1	2	3	4	–
Particle size (μm)	710–900	560–710	315–560	160–315	–
Stirring rate (s^{-1})	100	250	500	750	–

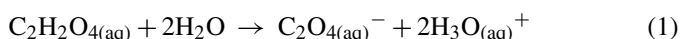
by volumetric method [16]. Experimental parameters used in the leaching process are given in Table 2.

3. Results and discussions

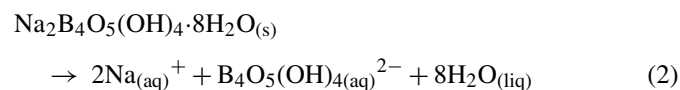
3.1. Leaching reactions

The leaching process of tincal in oxalic acid solution takes place according to the following reactions.

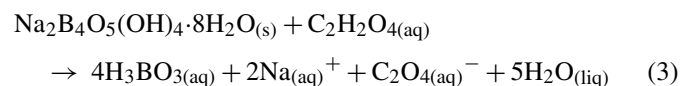
The oxalic acid solution is obtained as follows:



The leaching of tincal is as follows:



The overall reaction can be written as follows:



It was observed (Eq. (3)) that the reaction between tincal and oxalic acid resulted in boric acid and sodium oxalate in the liquid phase. After the tincal had been dissolved in the oxalic acid solution, it was cooled down to obtain a final crystal product. Furthermore, some solid materials were observed in the solution due to the impurities in tincal. The solid materials and filtrate crystals were analyzed by X-ray diffractometer (Figs. 2 and 3).

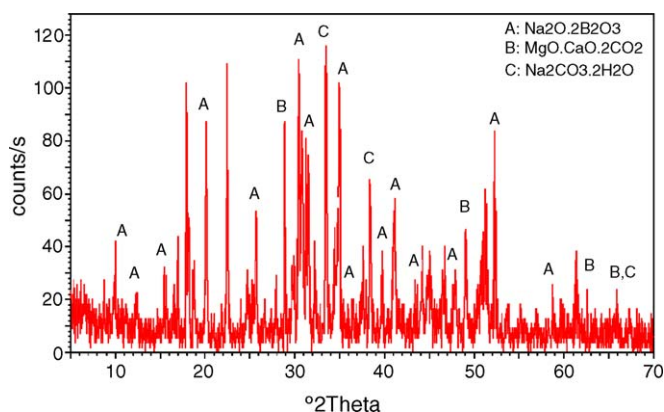


Fig. 1. X-ray diffractogram of tincal ore.

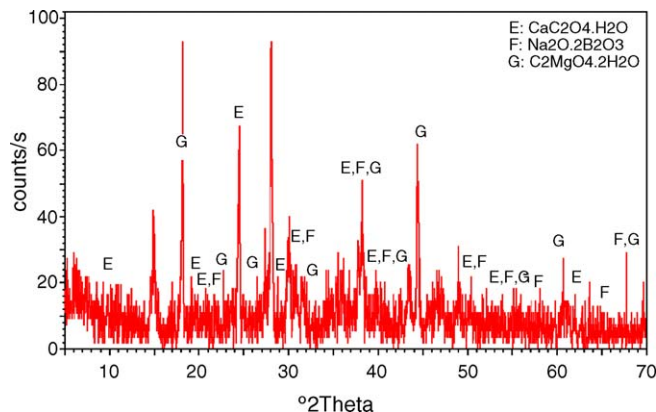


Fig. 2. X-ray diffractogram of solid materials on the filter paper.

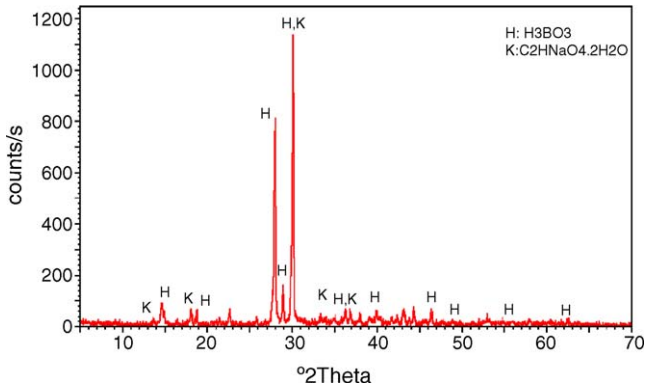


Fig. 3. X-ray diffractogram of filtrate crystals.

XRD analyses show that the solid materials consist of calcium oxalate, magnesium oxalate and undissolved tincal and the filtrate crystals consist of boric acid and sodium oxalate.

3.2. Effect of reaction temperature

The experiments were carried out at different temperatures. The results indicated that B₂O₃ concentration was reached 74.2% at 20 °C in 20 min. Maximum boron oxide leaching (99.0%) was obtained at 50 °C in 20 min. The leaching rate was observed to increase with increasing reaction temperature, (Fig. 4).

3.3. Effect of solid to liquid ratio

As seen in Fig. 5, after 20 min leaching time in the low solid to liquid ratio 74.2% B₂O₃ and in the high solid to liquid ratio 54.8% B₂O₃ was extracted. It was observed that as the solid to liquid ratio decreases, the leaching rate increases. This might be attributed to the fact that the amount of reagent compensation to every particle decreases with increasing solid amount in the suspension.

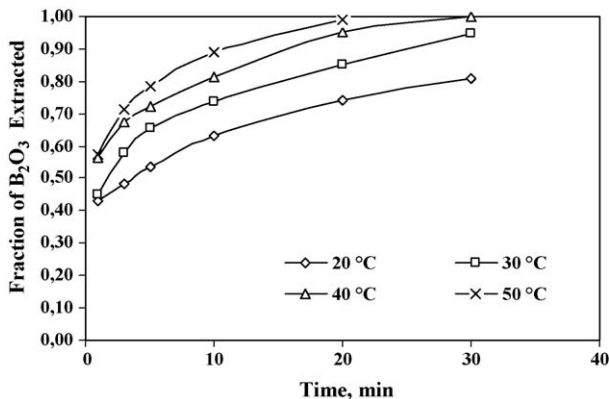


Fig. 4. Effect of reaction temperature on leaching of tincal (acid concentration, 1%; particle size, 315–560 μm; solid to liquid ratio, 1%; stirring speed, 500 s⁻¹).

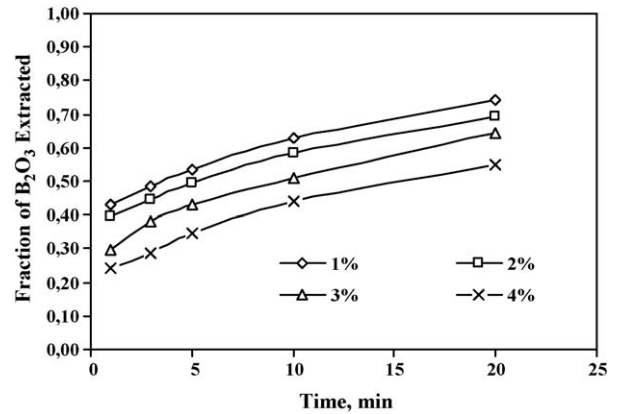


Fig. 5. Effect of solid to liquid ratio on leaching of tincal (acid concentration, 1%; temperature, 20 °C; particle size, 315–560 μm; stirring speed, 500 s⁻¹).

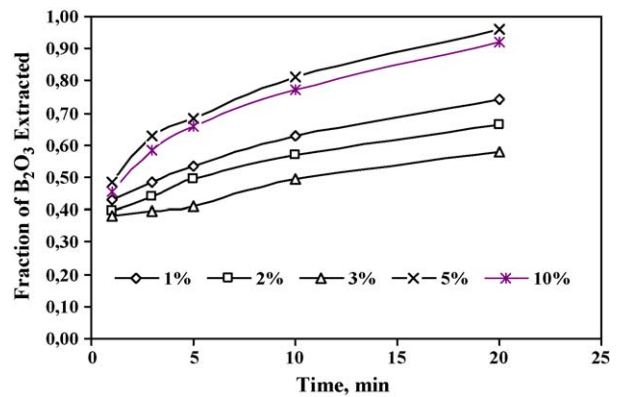


Fig. 6. Effect of acid concentration on leaching of tincal (particle size, 315–560 μm; temperature, 20 °C; solid to liquid ratio, 1%; stirring speed, 500 s⁻¹).

3.4. Effect of acid concentration

It was observed in the Fig. 6 that the B₂O₃ extraction was 74.2% in the low acid (1% w/v) concentration. However, as Fig. 7 shows, the extraction yield decreases as acid concentration increases from 1 to 3% and then increases as acid concentration

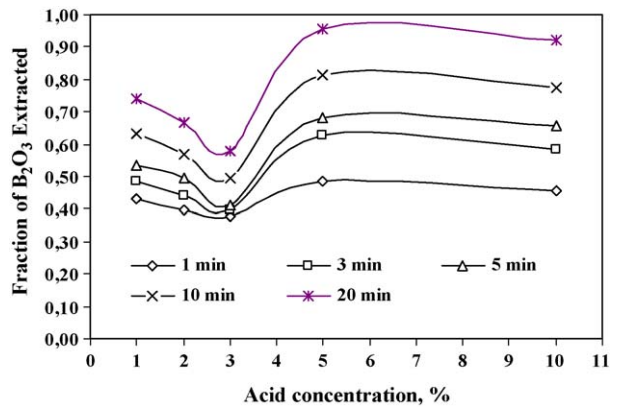


Fig. 7. Effect of acid concentration on leaching of tincal for 1–20 min (particle size, 315–560 μm; temperature, 20 °C; solid to liquid ratio, 1%; stirring speed, 500 s⁻¹).

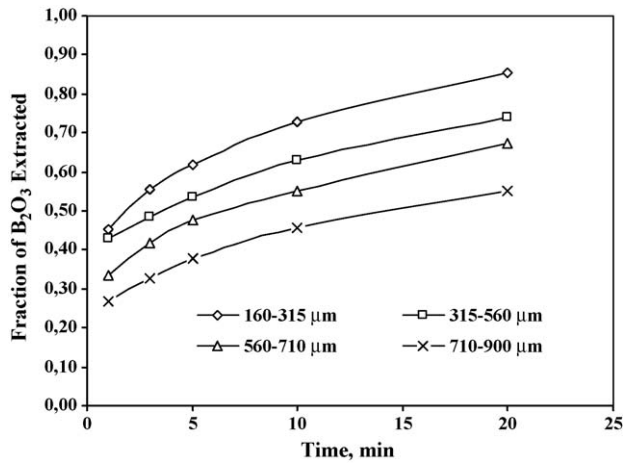


Fig. 8. Effect of particle size on leaching of tincal (acid concentration, 1%; temperature, 20 °C; solid to liquid ratio, 1%; stirring speed, 500 s⁻¹).

increases from 3 to 5%. At 5% acid concentration, the B₂O₃ extraction was 95.8%. Further increasing the acid concentration had no significant effect on the leaching fraction. Several studies showed similar results using colemanite dissolved in oxalic and acetic acid solutions [8,10]. The amount of theoretic acid was calculated as 0.24% at 1% solid to liquid ratio.

3.5. Effect of particle size

The results indicated that after 20 min leaching time 85.4% B₂O₃ was extracted for the fine particle size (160–315 μm). For the coarse particle size (710–900 μm), 55.2% B₂O₃ was extracted (Fig. 8). It is observed that the leaching rate increases with decreasing particle size. This can be attributed to the fact that as the particle size decreases the surface area of particles increases, which increases the contact area of particles with solution.

3.6. Effect of stirring speed

The effect of stirring speed on the leaching rate was investigated in the frequency range of 100–750 s⁻¹. The results showed that after 20 min leaching time, 54.8% of B₂O₃ in the low stirring speed and 68.4% of B₂O₃ in the high stirring speed was extracted. It is observed from Fig. 9 that the leaching rate increases with increasing stirring speed.

4. Kinetic analysis

The rate of reaction between a solid and fluid can be expressed in terms of the heterogeneous reaction models. The rate may be controlled by [17]:

- film diffusion control model;
- chemical reaction control model or
- product layer diffusion control model.

By applying the above models to the experimental data obtained in this study one find the kinetic mechanism in the

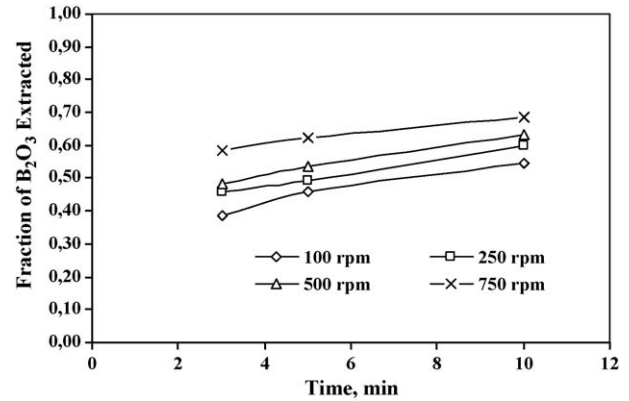


Fig. 9. Effect of stirring speed on leaching of tincal (acid concentration, 1%; particle size, 315–560 μm; solid to liquid ratio, 1%; temperature, 20 °C).

leaching process. Reaction time t , is given as a function of fractional leaching for surface chemical reaction control model, diffusion through fluid film control model, and diffusion product layer control model cases.

4.1. Film diffusion control model

The kinetics of film diffusion control model (A_1) is given by the following equation [17].

$$k_1 t = [x] \quad (4)$$

where k_1 is the reaction rate constant (min⁻¹), t the time (min), x is the fraction extracted. The leaching rates were calculated at various temperatures. The results were shown in Fig. 4. The results were also analysed by using the film diffusion control model given in Eq. (4) and x values were determined. The plot of $[x]$ versus time t at 20 °C is shown in Fig. 10. The film diffusion control model plot of $[x]$ versus time t does not produce a straight line. Therefore, this kinetic analysis showed that the process does not fit the film diffusion control model. The results were further analysed by the surface chemical reactions control model.

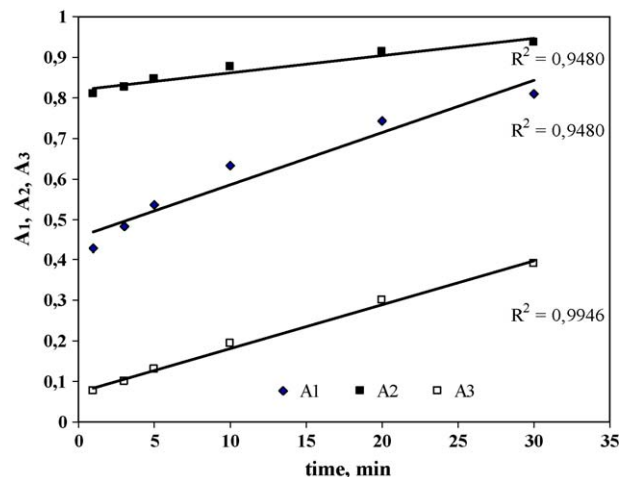


Fig. 10. The variation in A_1, A_2 and A_3 with time at temperature of 20 °C ($A_1 = x$; $A_2 = 1 - (1 - x)^{1/3}$; $A_3 = 1 - 3(1 - x)^{2/3} + 2(1 - x)$).

4.2. Surface chemical reactions control model

The kinetics of chemical reaction control model (A_2) is given by the following equation [17]:

$$k_2 t = [1 - (1 - x)^{1/3}] \quad (5)$$

where k_2 is the reaction rate constant (min^{-1}), t the time (min), x is the fraction extracted. The results were analyzed by using the surface chemical reactions control model given in Eq. (5) and $[1 - (1 - x)^{1/3}]$ values were calculated. The plot of $[1 - (1 - x)^{1/3}]$ versus time t at 20°C is shown in Fig. 10. The surface chemical reactions control model plots of $[1 - (1 - x)^{1/3}]$ versus time t did not produce a straight line. Therefore, this kinetic analysis showed that the process does not fit the surface chemical reactions control model. The results were further analysed by the product layer diffusion control model.

4.3. Product layer diffusion control model

The kinetics of product layer diffusion control model (A_3) is given by the following equation [17]:

$$k_3 t = [1 - 3(1 - x)^{2/3} + 2(1 - x)] \quad (6)$$

where k_3 is the reaction rate constant (min^{-1}), t the time (min), x is the fraction extracted. The results were also analysed by using the product layer diffusion control model given in Eq. (6) and $[1 - 3(1 - x)^{2/3} + 2(1 - x)]$ values were calculated.

The plot of $[1 - 3(1 - x)^{2/3} + 2(1 - x)]$ versus time t at 20°C is shown in Fig. 10. The product layer diffusion control model plots of $[1 - 3(1 - x)^{2/3} + 2(1 - x)]$ versus time t resulted in a straight line.

Furthermore, regression coefficients (R^2) were calculated for the three models. R^2 values were 0.9480 for the film diffusion control model, 0.9480 for the surface chemical reactions control model, and 0.9946 for the product layer diffusion control model.

The highest regression coefficient was observed in product layer diffusion control model. Therefore, product layer diffusion control mathematical model was chosen as the control model in this leaching process. The kinetics of product layer diffusion control model is shown in Fig. 11.

The rate constant values k_1 , k_2 and k_3 and correlation coefficients (R^2) for the three models were calculated at various temperatures from Eqs. (4)–(6). The results are given in Table 3. These results show that rate constants increases with increasing temperature for tincal leaching.

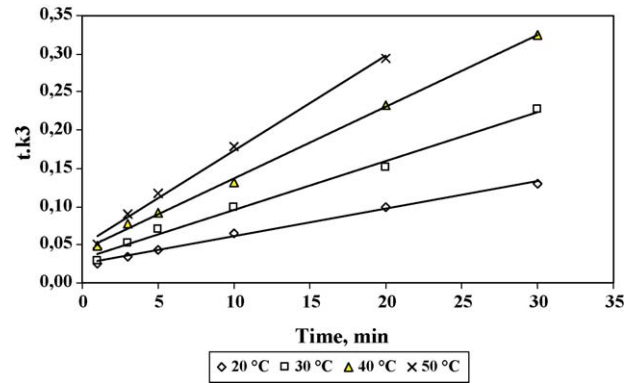


Fig. 11. The variation in $[1 - 3(1 - x)^{2/3} + 2(1 - x)]$ with time at various temperatures.

5. Activation energy

The temperature dependence of the chemical reactions can be given by the Arrhenius equation as follows:

$$\ln k_c = \ln A - \frac{E_a}{RT} \quad (7)$$

where k_c is the rate constant (cm min^{-1}), A the frequency factor, R the gas constant, T the temperature and E_a is the activation energy.

$$\text{rate constant is given as } k_c = \frac{k_3 \rho R^2}{6bC} \quad (8)$$

where k_3 is the reaction rate constant (min^{-1}) obtained from Eq. (6), C the concentration of oxalic acid (mol cm^{-3}), R the radius of particle (cm), ρ the density of tincal (mol cm^{-3}), and b is the stoichiometric coefficient of the solid.

According to Eq. (7), plot of $\ln k_c$ versus $1/T$ should be a straight line with a slope of $-E_a/R$ when experimental data follows Arrhenius equation (Fig. 12). Using chemical rate constant (k_3) from product layer diffusion control model fitted to the experimental data obtained in this study $\ln k_c$ values were calculated and $\ln k_c$ versus $1/T$ graph was plotted. From the slope of this graph the activation energy of tincal leaching in oxalic acid was found to be $35.14 \text{ kJ mol}^{-1}$. In a similar study Alkan [13] determined the activation energy of the ulexite in oxalic acid solutions as $30.69 \text{ kJ mol}^{-1}$.

Table 3
Values k_1 , k_2 , k_3 and R^2 of A_1 , A_2 and A_3 models at different temperatures

Temperature (K)	A_1		A_2		A_3	
	k_1 (min^{-1})	R^2	k_2 (min^{-1})	R^2	k_3 (min^{-1})	R^2
293	0.774	0.9480	0.528	0.9814	0.648	0.9946
303	0.912	0.9021	0.840	0.9819	1.158	0.9922
313	0.840	0.9069	1.308	0.9938	1.686	0.9983
323	1.200	0.8692	1.998	0.9930	2.526	0.9976

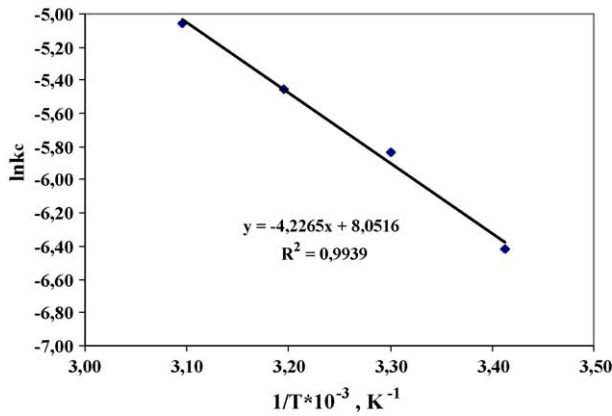


Fig. 12. Arrhenius plot for the leaching of tincal.

6. Conclusions

In this study, the leaching kinetics of tincal in oxalic acid solutions was investigated in a batch reactor. The results revealed that the leaching rate increases with increasing reaction temperature and stirring speed and decreasing solid to liquid ratio, and particle size. From the results the most important parameter on the leaching rate was found to be the temperature of the tincal while the least important parameter on the leaching rate was found to be the acid concentration.

Boric acid and sodium oxalate were produced by the leaching of tincal in oxalic acid. The formed boric acid and sodium oxalate passed into the filtrate. The calcium oxalate, magnesium oxalate and undissolved tincal remained on the filter paper as solid materials.

In this experiment tincal leaching kinetics was best described by the product layer diffusion control model. The activation energy of tincal in oxalic acid solution was calculated to be $35.14 \text{ kJ mol}^{-1}$.

References

- [1] C. Helvacı, A review of the mineralogy of the Turkish borate deposits, *Mercian Geol.* 6 (1978) 257–270.
- [2] W. Gerhartz, *Ullmann's Encyclopedia of Industrial Chemistry*, vol. A4, Germany, 1985.
- [3] R.B. King, R.B. Mcbroom, *Encyclopedia of Inorganic Chemistry*, vol. 1, John Wiley & Sons, New York, 1992.
- [4] R.A. Smith, R.B. Mcbroom, *Encyclopedia of Chemical Technology*, vol. 4, John Wiley, Canada, 1992.
- [5] M.M. Kocakerim, M. Alkan, Dissolution kinetics of colemanite in SO_2 saturated water, *Hydrometallurgy* 19 (1988) 385–392.
- [6] M. Alkan, M. Oktay, M.M. Kocakerim, Z. Karagölge, Dissolution kinetics of some borate minerals in CO_2 saturated water, *Hydrometallurgy* 26 (1991) 255–262.
- [7] C. Kum, M. Alkan, M.M. Kocakerim, Dissolution kinetics of calcined colemanite in ammonium chloride solution, *Hydrometallurgy* 36 (1994) 259–268.
- [8] C. Özmetin, M.M. Kocakerim, S. Yapıcı, A. Yartaşı, A semiempirical kinetic model for dissolution of colemanite in aqueous acetic acid solutions, *Ind. Eng. Chem. Res.* 35 (1996) 2355.
- [9] A. Künkül, S. Yapıcı, M.M. Kocakerim, M. Copur, Dissolution kinetics of ulexite in ammonia solutions saturated with CO_2 , *Hydrometallurgy* 441 (1997) 135–145.
- [10] M. Alkan, M. Doğan, Dissolution kinetics of colemanite in oxalic acid solutions, *Chem. Eng. Process.* 43 (2004) 867–872.
- [11] H. Temur, A. Yartaşı, M. Çopur, M.M. Kocakerim, The kinetics of dissolution of colemanite in H_3PO_4 solutions, *Ind. Eng. Chem. Res.* 39 (2000) 4114–4119.
- [12] C. Özmetin, M.M. Kocakerim, S. Yapıcı, A. Yartaşı, A semiempirical kinetic model for dissolution of colemanite in aqueous acetic acid solutions, *Ind. Eng. Chem. Res.* 35 (1996) 2355.
- [13] M. Alkan, M. Doğan, H. Namli, Dissolution kinetics and mechanism of ulexite in oxalic acid solutions, *Ind. Eng. Chem. Res.* 43 (2004) 1591–1598.
- [14] M. Tunc, S. Yapıcı, M.M. Kocakerim, A. Yartaşı, The dissolution kinetics of ulexite in H_2SO_4 solution, *Chem. Biochem. Eng. Q* 15 (2001) 175–180.
- [15] M. Tunc, Kocakerim, A. Yartaşı, A semi-empirical kinetic model for dissolution of ulexite in aqueous acetic acid, *Energy Educ. Sci. Technol.* 3 (1999) 1–10.
- [16] W.W. Scott, R.B. Mcbroom, *Standard Methods of Chemical Analysis*, vol. 1, D Van Nostrand, New York, 1963.
- [17] O. Levenspiel, *Chemical Reaction Engineering*, 2nd ed., Wiley, New York, 1972.